ARMY RESEARCH LABORATORY

Ballistic Penetration Phenomenology of High Symmetry Single Crystals

Pat W. Kingman
U.S. ARMY RESEARCH LABORATORY

Rodney A. Herring
ADVANCED RESEARCH LABORATORY

ARL-TR-700 February 1995

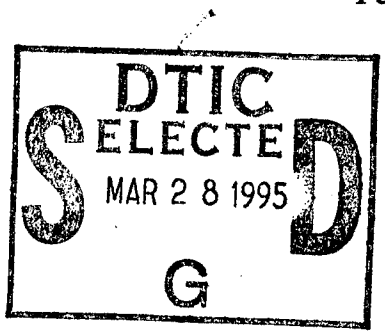

NOTICES

Destroy this report when it is no longer needed. DO NOT return it to the originator.

Additional copies of this report may be obtained from the National Technical Information Service, U.S. Department of Commerce, 5285 Port Royal Road, Springfield, VA 22161.

The findings of this report are not to be construed as an official Department of the Army position, unless so designated by other authorized documents.

The use of trade names or manufacturers' names in this report does not constitute endorsement of any commercial product.

REPORT DOCUMENTATION PAGE

Form Approved
OMB No. 0704-0188

1. AGENCY USE ONLY (Leave blank)	2. REPORT DATE	3. REPORT TYPE AND DATES COVERED
	February 1995	Final, March 89–March 90

4. TITLE AND SUBTITLE

Ballistic Penetration Phenomenology of High Symmetry Single Crystals

5. FUNDING NUMBERS

PR: 1L162618AH80

6. AUTHOR(S)

Pat W. Kingman and Rodney A. Herring*

7. PERFORMING ORGANIZATION NAME(S) AND ADDRESS(ES)

U.S. Army Research Laboratory
ATTN: AMSRL-WT-TD
Aberdeen Proving Ground, MD 21005-5066

8. PERFORMING ORGANIZATION REPORT NUMBER

9. SPONSORING/MONITORING AGENCY NAME(S) AND ADDRESS(ES)

U.S. Army Research Laboratory
ATTN: AMSRL-OP-AP-L
Aberdeen Proving Ground, MD 21005-5066

10. SPONSORING/MONITORING AGENCY REPORT NUMBER

ARL-TR-700

11. SUPPLEMENTARY NOTES

* Dr. Rodney A. Herring works for the Advanced Research Laboratory, Hitachi Limited, Hatoyama-machi, Hiki-gun, Saitama, Japan 350-03.

12a. DISTRIBUTION/AVAILABILITY STATEMENT

Approved for public release; distribution is unlimited.

12b. DISTRIBUTION CODE

13. ABSTRACT *(Maximum 200 words)*

The ballistic performance of tungsten single crystal penetrators is known to be a function of crystallographic symmetry. The macroscopic deformation geometry of both single crystal and polycrystal tungsten penetrators is a continuous eversion of the rod into a hollow tube. The differences in energy partitioning leading to these variations in ballistic performance must therefore be accounted for by detailed material deformation processes governed by crystallographic orientation. Inferences about these processes have been drawn from microstructural characterization of recovered penetrators.

Residual penetrators of both [011] and [111] orientations were found to have repeatedly deformed and recrystallized, but the actual operative processes led to quite different macrostructures, microstructures, and penetration depths. The [001] orientation deformed by a unique process which allowed very efficient deformation, resulting in maximum penetration depth.

These single crystal experiments demonstrate the critical role of detailed deformation processes in determining the final penetration depths even when similar macroscopic material flow geometry occurs.

14. SUBJECT TERMS

recrystallization, crystallization, deformation, microstructure, tungsten, single crystal, penetration, microstructure, deformation

15. NUMBER OF PAGES

20

16. PRICE CODE

17. SECURITY CLASSIFICATION OF REPORT	18. SECURITY CLASSIFICATION OF THIS PAGE	19. SECURITY CLASSIFICATION OF ABSTRACT	20. LIMITATION OF ABSTRACT
UNCLASSIFIED	UNCLASSIFIED	UNCLASSIFIED	UL

INTENTIONALLY LEFT BLANK.

ACKNOWLEDGMENT

The authors acknowledge the specimen preparation by David Mackenzie.

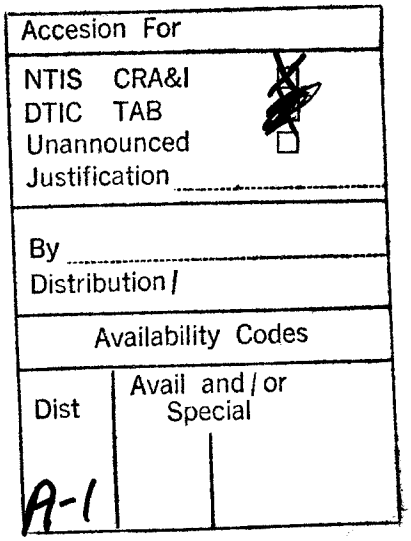

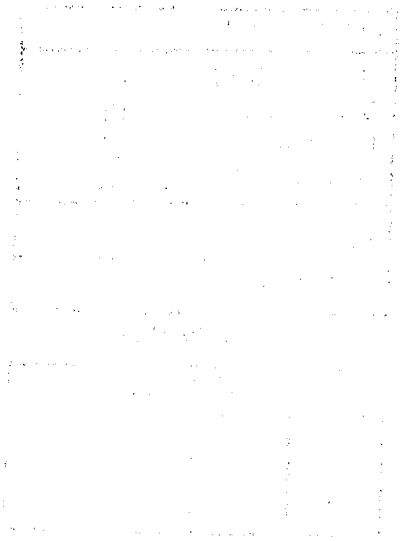

INTENTIONALLY LEFT BLANK.

TABLE OF CONTENTS

INTENTIONALLY LEFT BLANK.

LIST OF FIGURES

INTENTIONALLY LEFT BLANK.

1. INTRODUCTION

The material flow mechanisms which occur during ballistic penetration regimes and their role in influencing penetration behavior are not fully understood.

Penetration experiments at the U.S. Army Research Laboratory, in which tungsten single crystal rods of high symmetry orientations were fired into semi-infinite rolled homogenous armor (RHA) targets, showed that the penetration results were a strong function of crystallographic symmetry, and that the best performing orientation, the four-fold [100], exceeded current tungsten heavy alloy penetrators and was comparable to depleted uranium (Bruchey, Horwath, and Kingman 1991). Preliminary examination of recovered penetrators showed distinct differences in flow and failure patterns as a function of crystallography (Bruchey, Horwath, and Kingman 1991; Bruchey et al. 1992). The observed flow patterns are shown in Figure 1. These results are of fundamental interest because in single crystal experiments, all variations in geometry, ballistic conditions, and such material parameters as density, grain size, etc. are eliminated—crystallography is the single variable. Since the overall macroscopic deformation geometry in all cases is eversion of the rod into a continuous tube possessing a pattern of scroll-like foliations on the inner surface, the large differences in penetration must therefore arise from the crystallography of the detailed processes operating in the initiation and continuation of material flow in the lattice.

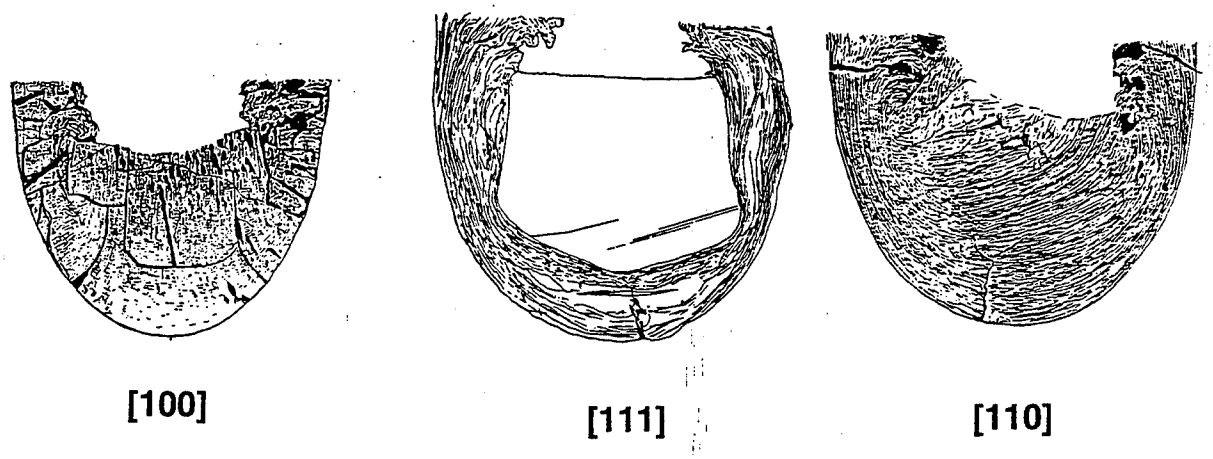

Figure 1. Geometry and flow patterns around nose of penetrators.

Preliminary characterization of the flow patterns and fracture topography of the post-mortem specimens has been further extended and now provides a basis for better understanding the mechanisms which influence the penetration performance.

2. EXPERIMENTAL APPROACH

A synergistic approach was applied to characterization, using optical metallography, scanning and transmission electron microscopy, and x-ray diffraction. The penetrators were embedded in semi-infinite RHA target blocks which were longitudinally sectioned. The residual back end of the penetrator, typically about one diameter (~6 mm) in length, rested at the bottom of the penetration cavity surrounded by a thin layer of flowed material which extended back along the cavity walls to form a continuous back-extruded tube 1–3 mm thick. Previous optical studies of these sections demonstrated the effects of crystallographic orientation on the general flow pattern during penetration and eversion (Bruchey, Horwath, and Kingman 1991; Bruchey et al. 1992) and provided a spatial reference frame for correlating microstructural information. The large size of the steel target block sections limited scanning microscopy of the fracture surfaces to examination of separated fragments, generally from the back-extrusion tubes. The unpolished halves of the sectioned targets were cut up and prepared for transmission microscopy. Transverse and longitudinal transmission electron microscopy (TEM) samples for each orientation were obtained by standard thinning techniques. X-ray diffraction patterns of the polished metallographic sections were used to determine the crystal orientation and provide lattice information at intermediate resolution. To characterize the small, inhomogeneous residual penetrator samples still embedded in massive blocks, Laue back reflection was the only feasible method. Although the irradiated area is comparatively large (about 0.5 mm), by making a series of small, incremental translations and comparing changes, the spatial resolution can be improved by about an order of magnitude. The target block was mounted in a special holder equipped with x and y micrometer translations. Once a reference point was established, relative positioning was extremely precise and reproducible and could be correlated directly with optical macros.

Information from white-radiation diffraction in necessarily qualitative but nonetheless Laue patterns can provide a wealth of information about a deformed sample: orientation, lattice inhomogeneity (bending, substructure, etc.), recrystallization, grain size, preferred orientation, etc. This information was a major key in drawing together all of the observations into a coherent picture of the deformation process.

3. RESULTS

3.1 Transmission Electron Microscopy. Dislocation arrangements were examined in samples of all three symmetry orientations, in both transverse and longitudinal sections, except for [110], where the only thinned sample obtained was transverse. More detailed discussion of the TEM results has been presented elsewhere (Bruchey et al. 1992), but the principal observations are summarized as follows.

The principal defect type observed was arrays of predominantly screw dislocations of the type b = 1/2 <111>. All crystals contained dislocation networks, subboundaries, and recrystallized grains, but the detailed dislocation arrangements varied as a function of crystallographic orientation. Dislocations observed in the [100] and [111] crystals were networks of pure screws or mixed dislocations with a large screw component. Dislocations in the [110] penetrator were straight screw dislocations with short segments left by edge dislocations. Other types of defects, such as twins and stacking faults, were not observed. There was often extensive recrystallization, with freshly recrystallized material adjacent to heavily deformed structures. However, due to the extreme inhomogeneity of the deformation, it was not possible to make direct correlation between the actual TEM observation area and the macrostructural flow pattern.

3.2 X-ray Diffraction. Observations for each orientation are summarized below.

3.2.1 [110] Penetrator. This residual penetrator was completely recrystallized except for a small region at one corner of the back end. The material in the etched band structure is polycrystalline, and Debye-Scherrer (D-S) rings from various regions showed a variety of substructures ranging from sharp, equiaxed recrystallized grains to broad cold-worked rings, generally with heavy texture. The few single crystal regions were distorted and ambiguous, and thus no orientation information could be obtained. Further examination showed that the rear surface of the rod was a jumble of irregular surfaces, implying that the residual rod was cracked irregularly throughout as suggested by the cracks visible in the macro-section.

3.2.2 [111] Penetrator. Diffraction patterns showed the clearly defined residual rod to be a single crystal, with little net lattice rotation except in the lobes near the front edge of the rod. Material in the flowed regions was primarily polycrystalline, with strong preferred orientation, but there were also included regions, primarily directly ahead of the residual rod, which were still single crystals, although severely bent and deformed (see Figure 2).

3.2.3 [100] Penetrator. The most salient factor in the [100] x-ray results was the persistence of single crystal character throughout the entire head of the penetrator and well into the extrusion tube. Optical macros showed no clearly outlined rod remnant, as seen in the [111] penetrator, but instead there was an assemblage of blocky segments defined by large cracks, and throughout much of the sample on a smaller

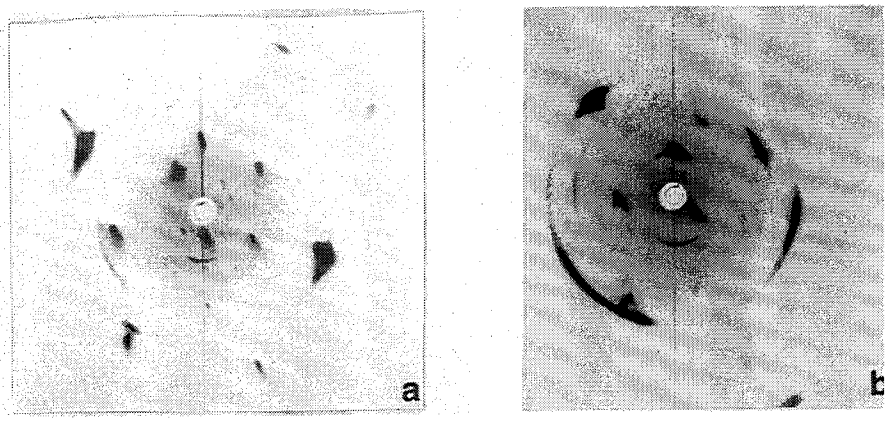

Figure 2. Diffraction patterns from [111]: (left) residual rod, (right) fragment embedded in recrystallized material ahead of residual rod.

scale there occurred a semicontinuous network of fine, straight crack segments intersecting at right angles. In the central residual rod, these cracks were parallel and perpendicular to the rod axis, but in the peripheral flow regions, they became respectively radial and parallel to the cavity interface.

X-ray analysis confirmed that the cracks were in all instances parallel to {100} cleavage planes. In the residual rod remnant, the diffraction pattern was always uniquely sharp and well-defined. Along the penetrator axis directly ahead of the residual rod, the orientation was maintained and the spots were uniformly broadened without asterism (see Figure 3). A traverse across the sample directly below the rod remnant showed the lattice orientation changing continuously, corresponding with the reorientation of the {010} cleavage cracks, with surprisingly little asterism except in the vicinity of major cracks (see Figure 4). Numerous sequences throughout the sample demonstrated that single crystal reflections were obtained except in the vicinity of a few obvious inhomogeneities such as the severe, localized bands found near the back edges of the penetrator, where local recrystallization occurred. Single crystal patterns from the immediate vicinity of major cracks or similar inhomogeneities sometimes contained twisted, forked, or ginko-leaf spot shapes, indicating complex local bending. Superimposed D-S rings from recrystallization might be seen, but in many other instances, uniform single-axis reorientation of the lattice occurred with a minimum of inhomogeneity (see Figure 5). These Laue patterns contained uniform, continuously extended spots. When both ends of each spot were plotted, two crystal orientations related by a single axis rotation were represented, giving the limits of the continuous lattice rotation occurring within the irradiated area.

Since the observation surface is an axial plane of the penetrator, continuous lattice reorientation about the normal to the observation plane is consistent with radial material flow. Along the left edge of the

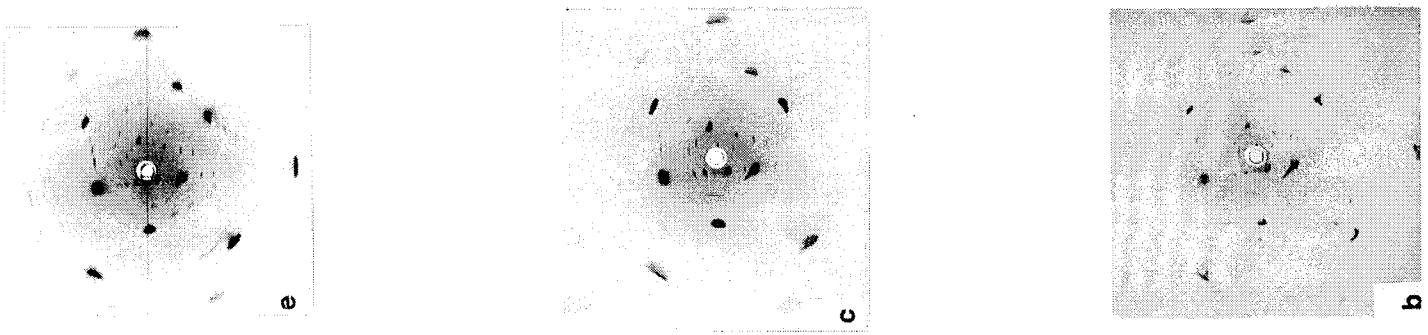

Figure 3. Diffraction patterns from [100]: (left) residual rod, (center, right) material ahead of residual rod.

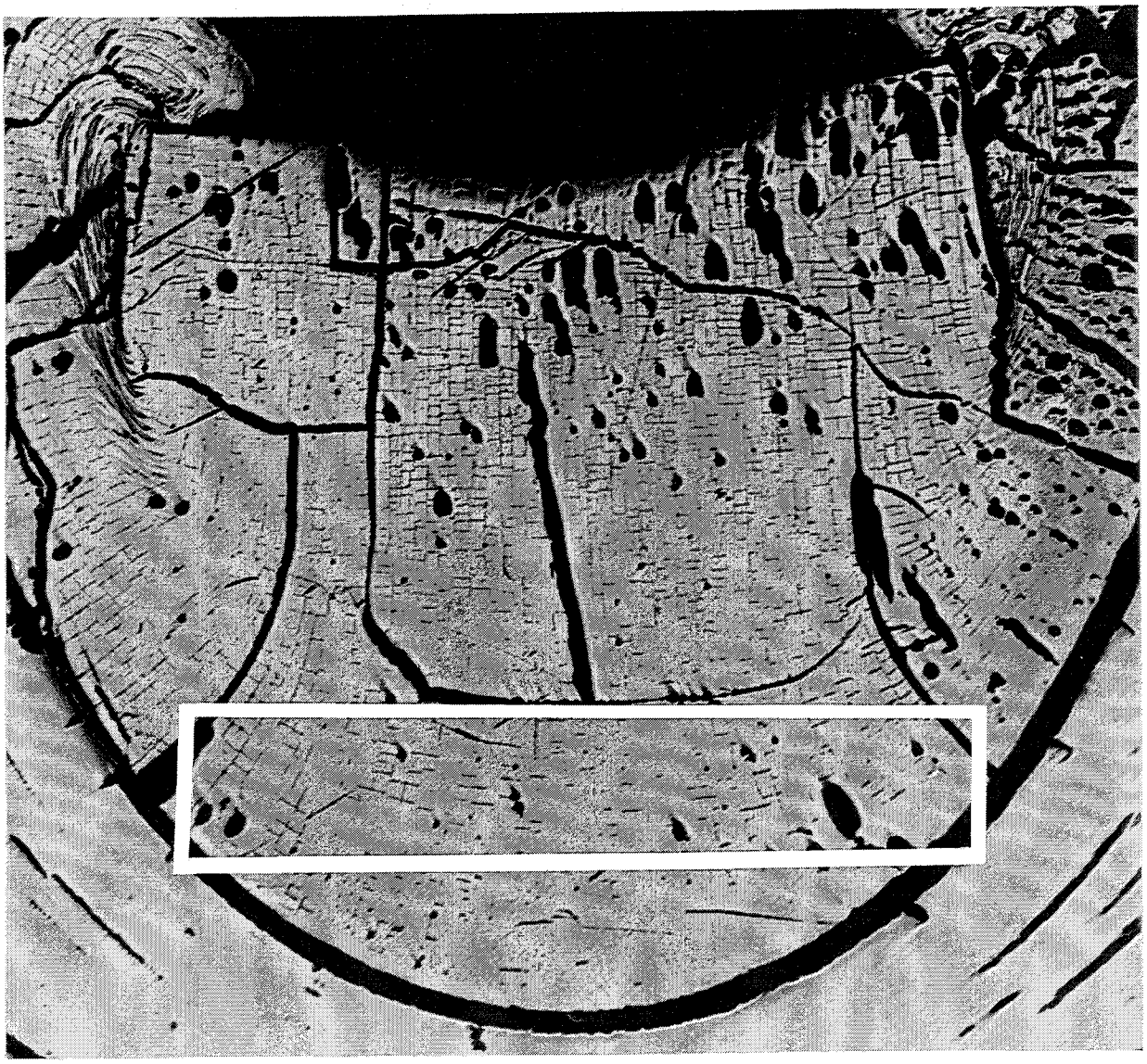

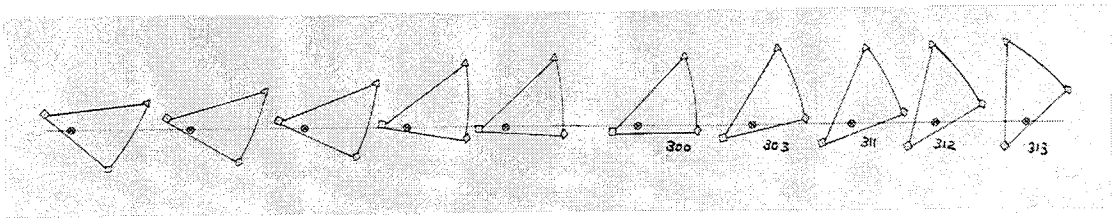

Figure 4. Stereograms of diffraction patterns taken in sequence across [100] peripheral flow, correlating with cleavage cracks.

penetrator, this lattice rotation can be documented continuously from the nose back into the hollow extrusion tube for several rod diameters without discontinuity, until the single crystal spots finally disappear in textured D-S patterns. Along the right edge, an orientation discontinuity occurs at a major crack near the residual rod, and a new orientation begins. Examination of a large fragment of another penetrator, which separated from the target block by fracturing away from a thin layer adhering to the cavity surface, clarified this discontinuity. Figure 6 shows the convex surface, partially covered with sheaf-like packets. X-rays of the packets showed broad, single crystal reflections along with D-S rings. Seen in three dimensions, these individual packets, defined by cleavage planes, appear to have sheared radially and also rotated in varying amounts about a normal axis. In agreement with the lattice rotations observed in the two-dimensional axial surface of the first penetrator.

4. DISCUSSION

From these observations, it is evident that the microstructural processes operative in these three single crystal penetrators are quite different.

In the [111] rod, three <111> directions occur symmetrically at 70.5° from the rod axis. Resolved shear stresses on these dislocations are thus relatively low, resulting in a high yield strength, while ample generation of dislocations available for interaction enhances work hardening. As well, screw dislocations will tend to move outward resulting in radial mass transfer toward the cavity walls. The well-defined character of the few narrow bands etched in the residual is undefined, but the location and direction, along with the presence of large crystal fragments surrounded by heavily deformed and recrystallized material just ahead of the residual rod, suggests that separation of discrete material segments initiates with these bands. Additionally, the inner surface of the penetration tunnel is wavy and pocked, suggesting radial impingement of discrete segments of penetrator material as the blunt nose of the remaining rod forces these segments radially outward and then between the rod and the cavity wall. Diffusion gradients at the penetrator surface and iron-rich intrusions in cracks appear only in this sample, implying higher temperatures than for the other orientations. Eventually the crystal segments recrystallize, perhaps repeatedly, with a strong preferred orientation. All of these processes absorb a fraction of the total energy, which thus becomes unavailable for forward penetration. Thus, the crystallographic factors which lead to high yield strength, work hardening, and superior stress strain characteristics in unconfined conventional testing actually detract from penetration performance.

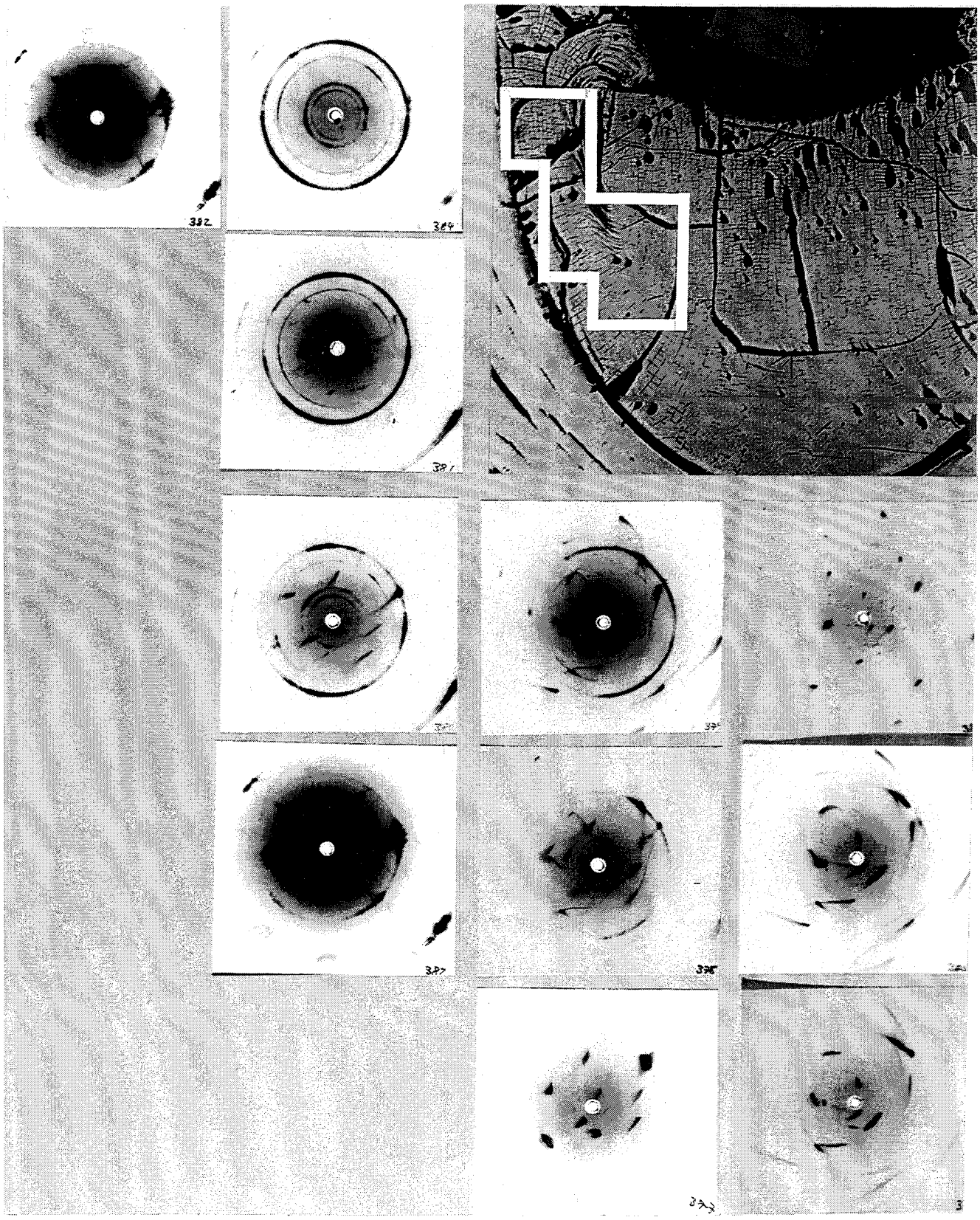

Figure 5. Diffraction patterns from adjacent regions in [100] residual penetrator.

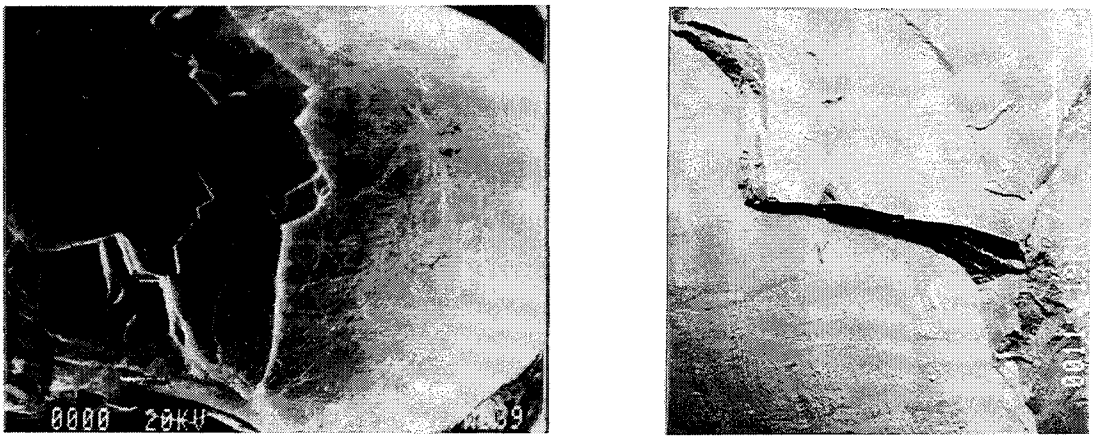

Figure 6. Convex surface of separated [100] residual penetrator.

In the [100] penetrator, the material mechanisms are different. With four-fold symmetry, all four <111> directions are equally stressed, creating large numbers of dislocations able to react with one another. One possible reaction (Carrington, Hale, and McLean 1960) is the Cottrell reaction:

$$\frac{1}{2}[\bar{1}1\bar{1}] + \frac{1}{2}[\bar{1}\bar{1}1] = [\bar{1}00],$$

which produces a sessile dislocation, as illustrated in Figure 7. Two slip dislocations combine to form a crack dislocation as indicated schematically in (A). The dislocation reaction given previously is shown in (B), with the resultant [001] sessile normal to the (001) plane. The cleavage crack nucleated by the sessile [001] is oriented as shown in (C) (Reed-Hill 1964). Under hydrostatic stresses, cracks would not open at once, but could be nucleated as deviatoric stresses increase and material flow is initiated. It can also be reasonably speculated that early creation of a large distribution of these sessiles would inhibit subsequent work hardening. The smooth lamellar bending and shear and the relative absence of substructure, complex lattice distortion, and recrystallization evident in x-ray patterns from much of the peripheral flow region indicate that the work hardening expected from standard stress-strain behavior does not occur. In contrast to the [111] penetration profile, the [100] penetration tunnel is narrow and exceptionally smooth, and there is little evidence of interaction between the penetrator and the target material. Rather than discontinuously shedding finite material segments, the [100] rod is postulated to flow by a smooth continuous process in which small, finite lattice elements defined by cleavage cracks

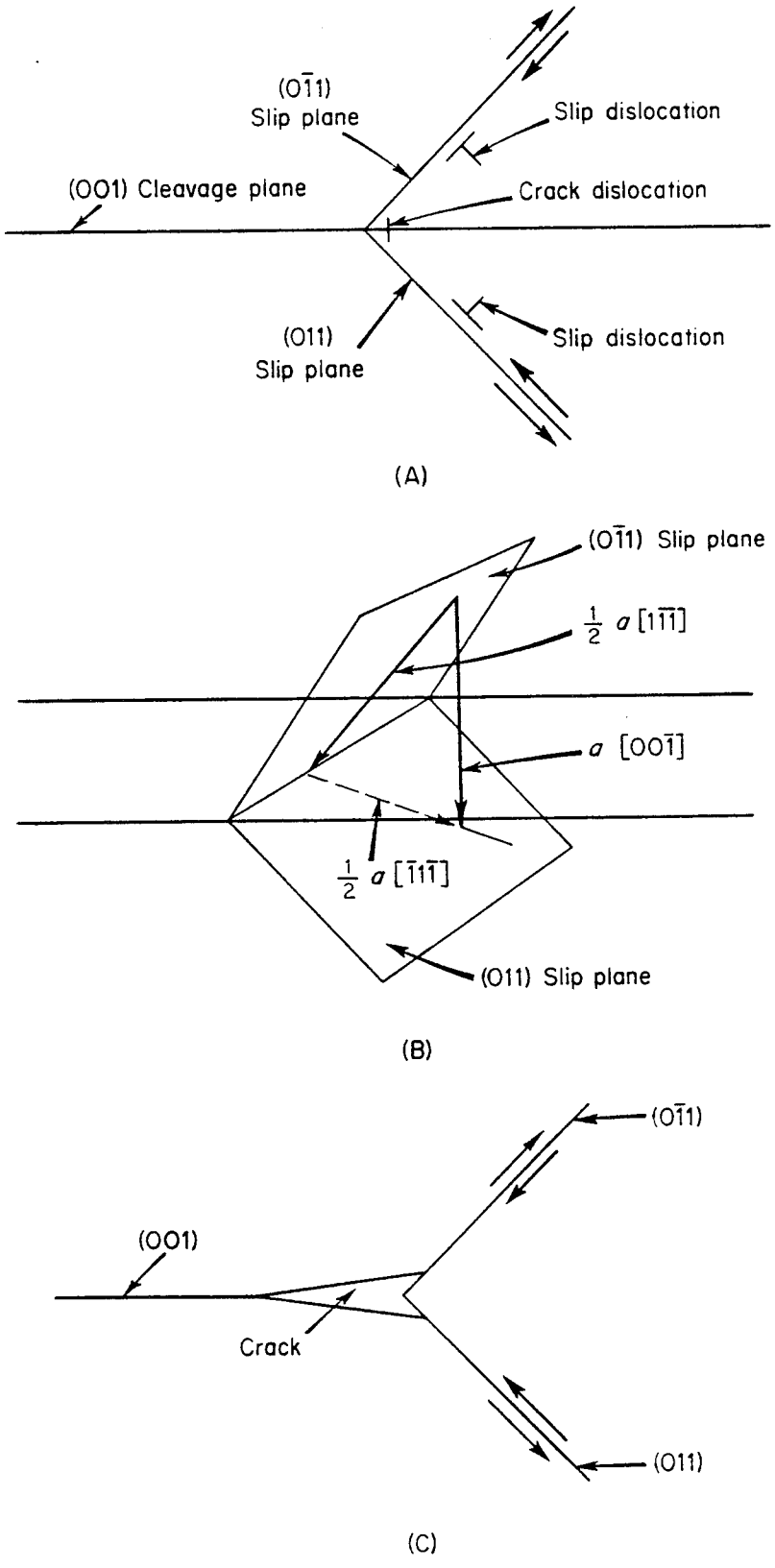

Figure 7. Cottrell's dislocation intersection mechanism for nucleation of {001} cracks, after Reed-Hill (1964).

undergo a combination of lamellar bending and rigid rotation with little internal disturbance—a process which is highly energy efficient, thus allowing maximum partition of energy into forward motion (i.e., penetration). Such features as the etched deformation bands at the back ends of the sample, which contain heavily deformed and recrystallized material, seem likely to be a localized artifact rather than a primary deformation mode. The persistence of the rectangular crack pattern even through the curved foliations in the extrusion tube (Figure 5) is strong evidence that lamellar flow of finite entities with minimal lattice disruption is the continuing deformation mode and that continuous reorientation of defined entities was complete before recrystallization eventually occurred.

Again, standard stress-strain properties do not predict penetration results, since the [100] yield and work-hardening curves are similar to but lower than those for [111], while in ballistic penetration a highly efficient alternative material flow mechanism occurs, absorbing less energy and allowing the [100] penetrator to exceed the performance of the [111].

For the [110] orientation, detailed conclusions are more difficult since the recrystallization is so extensive. In two-fold symmetry, only two <111> directions are stressed and work-hardening dislocation reactions are unavailable. Classically, [110] bcc crystals have a high yield but do not work harden; at high impact velocities, twins may occur (Subhash, Lee, Ravichandran 1994). The TEM, SEM, and x-ray results all indicate that the penetrator material has repeatedly recrystallized, deformed, and recrystallized again. The nature of the etched bands, which were entirely recrystallized with a strong preferred orientation, was not determined. The flow packets in the (110) extrusion tube were unique in having a completely non-crystallographic appearance; instead they resemble ductile, bifurcating fronds. It seems possible that multiple fractures occurred very early, and, after yield, ductile flow occurred with repeated recrystallization.

It is interesting to compare the observed modes occurring in single crystal rods with the work of Magness (1992) and Magness and Farrand (1991) in several materials. Magness interpreted these results in terms of the initiation of shear localizations, primarily adiabatic shear bands in the deforming penetrator. Figure 8, taken from Magness, shows schematically the flow patterns he identifies.

Mode (b), late shear localization and discard, leads to the mushrooming and wavy cavity profile resulting from nonsteady flow which are associated with poor penetration performance, and are typical of polycrystalline tungsten. The [111] flow pattern resembles this model: some mushrooming and a wavy

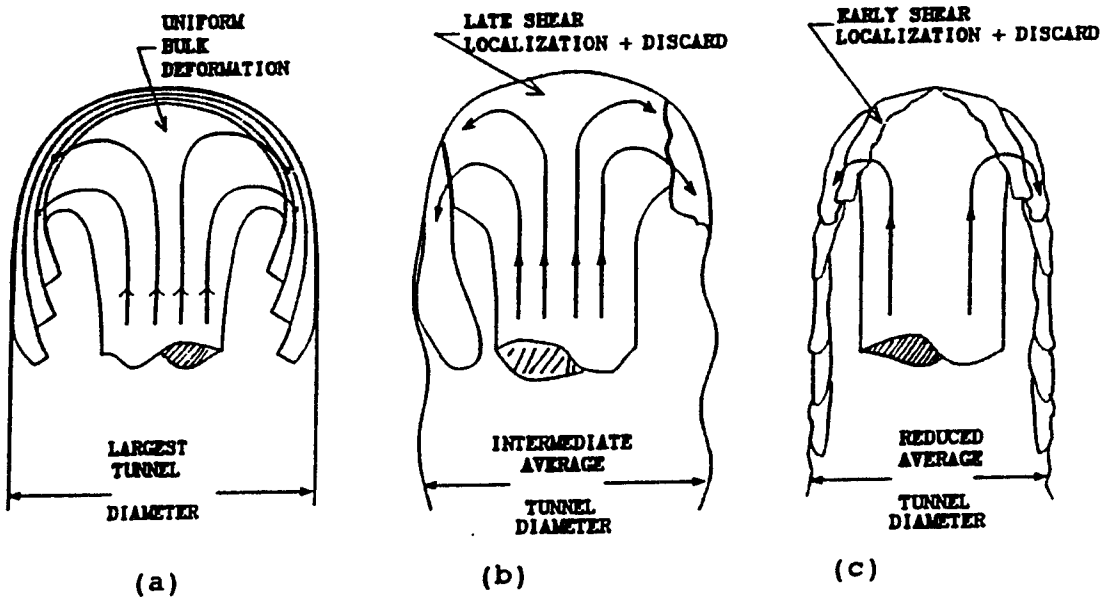

Figure 8. Schematic of postulated flow modes, after Magness (1992).

profile are definitely present, and the few narrow bands present may be sites for discontinuous material separation.

The penetration cavity of the [100] rod resembles mode (c), like that of the depleted uranium (DU) penetrators described by Magness. In the [100] case, the chisel-shape profile is absent, but the tip radius is still narrow and the geometry of the penetration tunnel resembles that of the early shear and discard model. It appears that the successful performance of this penetrator results from an extremely efficient flow mechanism initiated, like the adiabatic shear localizations observed in DU, early in the flow process, but on a much finer scale. This fine scale allows relatively smooth, continuous initiation of flow which is energetically efficient. Thus, the deformation mode occurring in the [100] crystal is an alternative mechanism which extends the concept of penetration by early initiation of energy-efficient shear to a microscopic scale.

The characterization of the [110] flow is less obvious, but the shallower, wider cavity with relatively smooth walls my be consistent with the stable, uniform flow model (a), modified by anisotropy. Further information about the actual flow mechanisms would be needed to characterize this orientation.

5. CONCLUSION

Single crystal penetrator tests have shown that crystallography, which governs microstructural failure and flow mechanisms, is a strong determinant of penetration behavior. Additionally, as previously pointed out by Magness and others, classical quasi-static data do not necessarily imply similar performance in ballistic penetration. Finally, the excellent performance of the [100] single crystal penetrators has been shown to result from a unique deformation mode in which work hardening is suppressed and flow initiates at microscopic inhomogeneities which allow small but finite crystal entities to shear and flow with minimal internal deformation. This mode allows an energetically efficient uniform flow which maximizes the fraction of total energy partitioned into forward penetration, resulting in a deep, narrow, smooth-walled penetration cavity similar to the geometry of "chisel nose" DU penetrators, but by a mechanism different from adiabatic shear. Single crystal experiments provide a unique opportunity to isolate the effects of crystal symmetry on microstructural deformation and study the basic material mechanisms involved. This understanding will lead to more effective processing to use and optimize the appropriate properties of existing materials and can ultimately define a basis for designing novel materials and composites in the future.

INTENTIONALLY LEFT BLANK.

6. REFERENCES

Bruchey, W. J., R. A. Herring, P. W. Kingman, and E. J. Horwath. "Deformation Mechanisms in Tungsten Single Crystals in Ballistic Impact Experiments." High Strain Rate Behavior of Refractory Metals and Alloys, Asfahnai et al. (eds.), Warrendale, PA: TMS, 1992.

Bruchey, W. J., E. J. Horwath, and P. W. Kingman. "Orientation Dependence of Deformation and Penetration Behavior of Tungsten Single-Crystal Rods." Tungsten and Tungsten Alloys, Recent Advances, A. Crowson and E. Chen (eds.), Warrendale, PA: TMS, 1991

Carrington, W., K. F. Hale, and D. McLean. "Arrangement of Dislocations in Iron." Proc. Roy. Sci. A, vol. 259, pp. 203–227, 1960.

Magness, L. S. "Properties and Performance of KE Penetrator Materials." Tungsten and Tungsten Alloys, Metal Powder Industries Federation, pp. 15–22, Princeton, NJ, 1992.

Magness, L. S., and T. S. Farrand. "Deformation Behaviour and Its Relationship to the Penetration Performance of High-Density KE Penetrator Materials." Proceedings of the 1990 Army Science Conference, pp. 465–479, 1991.

Reed-Hill, R. Physical Metallurgy Principles. Van Nostrand, pp. 534–536, Princeton, NJ, 1964.

Subhash, G., Y. J. Lee, and G. Ravichandran. "Plastic Deformation of CVD Textured Tungsten." Acta Metallurgica, vol. 42, pp. 319–330, 1994.

INTENTIONALLY LEFT BLANK.

NO. OF COPIES	ORGANIZATION
2	ADMINISTRATOR ATTN DTIC DDA DEFENSE TECHNICAL INFO CTR CAMERON STATION ALEXANDRIA VA 22304-6145
1	COMMANDER ATTN AMCAM US ARMY MATERIEL COMMAND 5001 EISENHOWER AVE ALEXANDRIA VA 22333-0001
1	DIRECTOR ATTN AMSRL OP SD TA US ARMY RESEARCH LAB 2800 POWDER MILL RD ADELPHI MD 20783-1145
3	DIRECTOR ATTN AMSRL OP SD TL US ARMY RESEARCH LAB 2800 POWDER MILL RD ADELPHI MD 20783-1145
1	DIRECTOR ATTN AMSRL OP SD TP US ARMY RESEARCH LAB 2800 POWDER MILL RD ADELPHI MD 20783-1145
2	COMMANDER ATTN SMCAR TDC US ARMY ARDEC PCTNY ARSNL NJ 07806-5000
1	DIRECTOR ATTN SMCAR CCB TL BENET LABORATORIES ARSENAL STREET WATERVLIET NY 12189-4050
1	DIR USA ADVANCED SYSTEMS ATTN AMSAT R NR MS 219 1 R&A OFC AMES RESEARCH CENTER MOFFETT FLD CA 94035-1000

NO. OF COPIES	ORGANIZATION
1	COMMANDER ATTN AMSMI RD CS R DOC US ARMY MISSILE COMMAND REDSTONE ARSNL AL 35898-5010
1	COMMANDER ATTN AMSTA JSK ARMOR ENG BR US ARMY TANK AUTOMOTIVE CMD WARREN MI 48397-5000
1	DIRECTOR ATTN ATRC WSR USA TRADOC ANALYSIS CMD WSMR NM 88002-5502
1	COMMANDANT ATTN ATSH CD SECURITY MGR US ARMY INFANTRY SCHOOL FT BENNING GA 31905-5660
	ABERDEEN PROVING GROUND
2	DIR USAMSAA ATTN AMXSY D AMXSY MP H COHEN
1	CDR USATECOM ATTN AMSTE TC
1	DIR USAERDEC ATTN SCBRD RT
1	CDR USACBDCOM ATTN AMSCB CII
1	DIR USARL ATTN AMSRL SL I
5	DIR USARL ATTN AMSRL OP AP L

NO. OF COPIES	ORGANIZATION
1	HQDA ATTN SARD TT DR F MILTON WASHINGTON DC 20310-0103
1	HQDA ATTN SARD TT MR J APPEL WASHINGTON DC 20310-0103
2	COMMANDER US ARMY ARDEC ATTN SMCAR AET M B TANNER D KAPOOR PICATINNY ARSENAL NJ 07806-5000
2	DIR US ARMY RESEARCH LABORATORY ATTN AMSRL MA MB R DOWDING P SMOOT WATERTOWN MA 02172-0001
2	DIR US ARMY RESEARCH LABORATORY ATTN AMSRL MA MA R ADLER M WELLS WATERTOWN MA 02172-0001
1	DIR US ARMY RESEARCH LABORATORY ATTN AMSRL MA CA WATERTOWN MA 02172-0001
1	DIR US ARMY RESEARCH LABORATORY ATTN AMSRL MA OB D SNOHA WATERTOWN MA 02172-0001
4	DIR US ARMY RESEARCH LABORATORY ATTN AMSRL MA PD S CHOU J DANDEKAR T WECRASOORIYA A RAJENDRAN WATERTOWN MA 02172-0001
2	DIR LOS ALAMOS NATL LABORATORY ATTN A D ROLLER MAIL STOP G 700 B HOGAN MAIL STOP F 681 PO BOX 1663 LOS ALAMOS NM 87545

NO. OF COPIES	ORGANIZATION
2	DIRECTOR SANDIA NATIONAL LABORATIES ATTN DR D E GRADY DR E S HERTEL ALBUQUERQUE NM 87185-5800
2	UNIVERSITY OF CALIFORNIA SAN DIEGO ATTN PROF KENNETH VECCHIO PROF MARC MEYER DEPT OF APPLD MECHS & ENGRG SCI B 010 LA JOLLA CA 92093
2	THE JOHNS HOPKINS UNIVERSITY ATTN PROF B GREEN PROF J WINTER MARYLAND HALL 34TH & CHARLES ST BALTIMORE MD 21218
2	THE JOHNS HOPKINS UNIVERSITY ATTN DR K T RAMESH DR K HEMKER LATROBE 104 34TH & CHARLES ST BALTIMORE MD 21218
1	BROWN UNIVERSITY ATTN PROF R CLIFTON DIVISION OF ENGINEERING PROVIDENCE RI 02912
1	ADLEMAN ASSOCIATES ATTN CARL CLINE 3301 EL ALIMO RIAL SUITE 280 ATHERTA CA 94027
1	FAILURE ANALYSIS ASSOCIATES ATTN MR STEPHEN ANDREWS ENGRG AND SCIENTIFIC SERVICES PO BOX 3015 149 COMMONWEALTH DR MENLO PARK CA 94025
1	MICHIGAN TECHNICAL UNIVERSITY ATTN G SUBHASH DEPT OF MECHANICAL ENGINEERING HOUGHTON MI 49931
2	BATTELLE PACIFIC NORTHWEST LABORATORIES ATTN W GURWELL G DUDDER RICHLAND WA 99352

NO. OF COPIES	ORGANIZATION
	ABERDEEN PROVING GROUND, MD
19	DIR USARL ATTN AMSRL WT PA W A LEONARD AMSRL WT PD B P BURNS AMSRL WT T T W WRIGHT AMSRL WT TA W J BRUCHEY G L FILBEY W J GILLICH E J HORWATH D E MACKENZIE E J RAPACKI W R ROWE AMSRL WT TC F I GRACE L S MAGNESS E H WALKER AMSRL WT TD A M DIETRICH K FRANK P W KINGMAN M J SCHEIDLER J W WALTER AMSRL WT WD L J KECSKES

INTENTIONALLY LEFT BLANK.

USER EVALUATION SHEET/CHANGE OF ADDRESS

This Laboratory undertakes a continuing effort to improve the quality of the reports it publishes. Your comments/answers to the items/questions below will aid us in our efforts.

1. ARL Report Number ARL-TR-700 Date of Report February 1995

2. Date Report Received _____

3. Does this report satisfy a need? (Comment on purpose, related project, or other area of interest for which the report will be used.) _____

4. Specifically, how is the report being used? (Information source, design data, procedure, source of ideas, etc.) _____

5. Has the information in this report led to any quantitative savings as far as man-hours or dollars saved, operating costs avoided, or efficiencies achieved, etc? If so, please elaborate. _____

6. General Comments. What do you think should be changed to improve future reports? (Indicate changes to organization, technical content, format, etc.) _____

CURRENT ADDRESS

_____
Organization

_____
Name

_____
Street or P.O. Box No.

_____
City, State, Zip Code

7. If indicating a Change of Address or Address Correction, please provide the Current or Correct address above and the Old or Incorrect address below.

OLD ADDRESS

_____
Organization

_____
Name

_____
Street or P.O. Box No.

_____
City, State, Zip Code

(Remove this sheet, fold as indicated, tape closed, and mail.)
(DO NOT STAPLE)

DEPARTMENT OF THE ARMY

OFFICIAL BUSINESS

NO POSTAGE
NECESSARY
IF MAILED
IN THE
UNITED STATES

BUSINESS REPLY MAIL
FIRST CLASS PERMIT NO 0001,APG,MD

POSTAGE WILL BE PAID BY ADDRESSEE

DIRECTOR
U.S. ARMY RESEARCH LABORATORY
ATTN: AMSRL-WT-TD
ABERDEEN PROVING GROUND, MD 21005-5066